

On Hofstadter butterfly spectrum: Chern-Simons theory, subband gap mapping, IQHE and FQHE labelling

F. A. Buot^{1,2,3}, G. Maglasang^{1,3}, A. R. Elnar^{1,3} and C. M. Galon^{1,3}

¹CTCMP, Cebu Normal University, Cebu City 6000
Philippines,

²C&LB Research Institute, Carmen, Cebu 6005
Philippines,

³LCFMNN, University of San Carlos, Cebu City 6000,
Philippines

October 19, 2021

Abstract

The magnetic field affects the Bloch band structure in a couple of ways. First it breaks the Bloch band into magnetic subbands or the Landau levels are broadened into magnetic Bloch bands. The resulting group of subbands in the central portion of the energy scale is associated with the integer quantum Hall effect (IQHE). Then at high fields it changes the integrated density of states of the remaining lowest and topmost subband, respectively, which can be associated with fractional quantum Hall effect (FQHE).

Here, we employ the Maxwell Chern-Simons gauge theory to formulate the subband-gap mapping algorithm and to construct the butterfly profile of the Hofstadter spectrum. The two regions in the spectrum responsible for the IQHE are identified. At very high magnetic fields the highest and lowest subband are affected by magnetic-field induced restructuring of the integrated density of states in each subband, respectively. The resulting transformation of each of the two subband is responsible for the FQHE. Thus, in the central regions of the energy scale, the principal group of subbands defined by the gap mapping is responsible for the IQHE. The fine structure of the topmost and lowest subband, which convey an iterative nature of the magnetic spectrum is a result of a hierarchical scaling and restructuring by the magnetic fields on the integrated density of states in each respective subband and is responsible for the FQHE.

1 INTRODUCTION

When electrons are subjected to both a magnetic field and a periodic electrostatic potential, two-dimensional systems of electrons exhibit a complex energy spectrum, known as the Hofstadter's butterfly [1]. This complex spectrum results from an incommensurate/commensurate interplay between two characteristic length scales, defined by the magnetic lattice with lattice constant given by the magnetic length, l_B , and the periodic electrostatic potential with lattice constant denoted by a . The magnetic length l_B has the physical meaning of the smallest size of a circular orbit in a magnetic field which is allowed by the uncertainty principle. Following Hofstadter [1] and Wannier [2], we assume the square lattice model with the two quantizing fields which perhaps yield the first fractal-like energy spectrum discovered in physics.

The Schrödinger difference equation studied by Hofstadter[1] is known as the Harper's equation and can be written as

$$u(m+1) + u(m-1) + 2 \cos \left(m \left(\frac{2\pi}{n} \right) - v \right) u(m) = \epsilon u(m) \quad (1)$$

where m and n are integers. We shall see that n denotes the number of magnetic subbands in what follows. Obviously, this equation has periodicity in $\Phi = \frac{2\pi}{n}$. The energy spectrum obtained[1] is shown in Fig. 1

To explain the above complex spectrum, Wannier [2], using counting arguments, derived the so-called Diophantine equation to map out the energy subband gaps of the spectrum. Here, we propose a simpler counting argument.

We employ the Maxwell Chern-Simons (CS) gauge theory[3, 4] to start the counting arguments for subband gap mapping. First we set the basic variables in analyzing the complex spectrum using CS gauge theory. Acknowledging the symmetry and periodicity of the complex energy spectrum shown in Fig. 1, we then draw the lines defining the bottom and top of the subbands, i.e, the subband gaps. Our results is depicted in Fig. 2 and Fig. 3. These figures will be discussed in more detail in what follows.

More of the lines are drawn in Fig.3 to show how the rays, defining different values or numeration counting of the subbands emanates from the four corners of the spectrum.

2 MAXWELL CHERN-SIMONS GAUGE THEORIES

We write the Chern-Simons Lagrangian density for $U(1)$ gauge theory for 2-dimensional system of manifold, M , as

$$\mathcal{L}_{CS} = \gamma \epsilon^{\mu\lambda\nu} A_\mu \partial_\lambda A_\nu - A_\mu J^\mu \quad (2)$$

where $J^\mu = (\rho, \vec{J})$, ρ is the charge density and \vec{J} is the current density. Later, we will associate the parameter γ with our magnetic parameters. Equation (2)

is often referred to as the Maxwell Chern-Simons theory [4]. The equation of motion is obtained by variation with respect to A_μ

$$\frac{\delta \mathcal{L}_{CS}}{\delta A_\mu} = \gamma \varepsilon^{\lambda\nu} \partial_\lambda A_\nu - J^\mu = 0$$

This gives

$$\gamma \int_M \nabla \times \vec{A} \cdot d\vec{a} = \int_M J^0 = \int_M \rho \quad (3)$$

$\int_M \rho$ is equal to the integrated density of states of each subband. In general, each subband have the same integrated density of states, reflecting the same degeneracy for each Landau levels in free electrons case.

We now show that the total density of states is an integer, equal to the magnetic flux divided by the quantum flux, which is equal to the degeneracy of a Landau level in a magnetic field. We do this by first counting the number of states in magnetic phase-space. This is given by [3]

$$\begin{aligned} \mathcal{N} &= \frac{1}{2\pi\hbar} \iint \vec{\nabla} \times \vec{\mathcal{K}} \cdot d\vec{a} \\ &= \frac{1}{2\pi\hbar} \iint \vec{\nabla} \times \frac{e}{c} \vec{A} \cdot d\vec{a} \end{aligned}$$

where $\vec{\mathcal{K}} = \vec{P} + \frac{e}{c} \vec{A} + \vec{F}ct$, [5] Φ is the total magnetic flux, and \vec{F} is the uniform electric field. We will ignore the electric field from now on. Therefore, the Landau level degeneracy, \mathcal{N} , is

$$\begin{aligned} \mathcal{N} &= \frac{1}{2\pi\hbar} \frac{e}{c} \iint \vec{B} \cdot d\vec{a} \\ &= \frac{\Phi}{2\pi \left(\frac{\hbar c}{e}\right)} = \frac{\Phi}{\phi_o} \end{aligned}$$

where $\left(\frac{2\pi\hbar c}{e}\right) = \phi_o$ is the quantum flux. For a square lattice, the number of quantum states in one Bloch band is equal to the number of lattice sites, N . We denote by n the number of magnetic subband formed from a Bloch band under a uniform magnetic field. Since the magnetic field does no work or does not impart energy on the systems, we can assume that the number of quantum states in a Bloch band is conserved when uniform magnetic field is applied. Thus for n subbands, we have,

$$\begin{aligned} N &= \frac{n}{2\pi\hbar} \iint \vec{\nabla} \times \frac{e}{c} \vec{A} \cdot d\vec{a} = n \frac{Na^2}{2\pi (l_B)^2} \\ &= n \frac{\Phi}{\phi_o} \end{aligned} \quad (4)$$

In other words,

$$n = \frac{N}{\left(\frac{\Phi}{\phi_o}\right)} = \frac{N}{\mathcal{N}}$$

where the Landau level (LL) degeneracy \mathcal{N} is,

$$\mathcal{N} = \left(\frac{\Phi}{\phi_o} \right)$$

Thus, we can measure the whole Bloch band in units of the LL degeneracy to give us the number of subbands. We end up with

$$n \frac{Na^2}{2\pi(l_B)^2} = N \quad (5)$$

where $\mathcal{N} = \frac{Na^2}{2\pi(l_B)^2}$ is the degeneracy of each subband, a is the lattice constant of a 2-D square lattice and $l_B = \sqrt{\frac{\hbar c}{eB}}$. Putting $N = 1$ or cancelling on both sides of Eq. (5), we have effectively normalized our Bloch band width to unity.

We redefine our flux variable as

$$\Phi = \frac{a^2}{2\pi(l_B)^2} = \frac{1}{n}, \quad 0 \leq \frac{1}{n} \leq 1,$$

Then we have

$$n = \frac{1}{\frac{a^2}{2\pi(l_B)^2}} = \frac{1}{\Phi} \quad (6)$$

In Eq. (6), the number of subbands is determined in units of Φ . We see that our normalized Bloch band is now measured in units of Φ . We see that when $\Phi = 1$, the magnetic lattice coincides with the periodic atomic potential lattice, and hence one expects that a single Bloch band is restored, $E(k)$ is periodic in k and in reduced Brillouin zone or one band, $0 \leq k \leq \frac{2\pi}{a} = \frac{2\pi}{l_B}$ with l_B the magnetic length, i.e., consisting of only one subband equal to the whole Bloch band width.

3 SUBBAND GAP MAPPING

In tracing the first gap from the top of the Bloch band width, we reckon that the *bottom* of the first gap from the *topmost* first subband must lie at values of one value of Φ down in the Bloch energy-band scale. This will define the diagonal line given by the linear equation,

$$W_{bottom} = 1 - \Phi$$

starting from (0, 1) coordinate, where W is the 'y-coordinate' representing the points in the normalized zero-field Bloch band width. Other subbands *bottom* boundaries will be defined by lines given by the linear equation,

$$W_t = 1 - t\Phi, \quad t \leq n, t \text{ integer}$$

starting from (0, 1) coordinate, where n is the total number of subbands.

On the other hand, *top* boundary of the *lowest* subband must lie after a one count of Φ . This define another diagonal line of a linear equation,

$$W_{toplow} = \Phi$$

stating from $(0, 0)$ coordinate. These diagonal lines are depicted in Figs. 1 and 2. Other subbands top boundaries will be defined by lines given by the linear equation,

$$W_l = l\Phi, \quad l \leq n, \quad l \text{ integer}$$

stating from $(0, 0)$ coordinate.

3.1 Reflection symmetry at $\Phi = \frac{1}{2}$

The Hofstadter butterfly spectrum is somewhat reminiscent of a Cantor set, which is an example of *fractal* string. In Fig.4, the horizontal line may represent the zero-field Bloch band width. By tentatively identifying the Hofstadter butterfly spectrum with the cantor set, we see that the limiting lowest number of subbands is $n \geq 2$. Physically of course, the lower integer value $n = 1$ just coincide with the original zero-field Bloch band width. Just like the Cantor set the gap between the limiting two subbands is the largest in the set. This is also physically meaningful since at this magnetic field strength the flux is large, or the degeneracy is large and concentrated in the two subbands. Moreover, the cyclotron frequency spacing, $\hbar\omega = \frac{eB}{mc}$, is also large and the two subbands are located symmetrically near the middle of the zero-field Bloch band width. Since $n = \infty$ and $n = 1$ are physically identical, giving the whole zero-field Bloch band width at this limiting cases, while also considering the periodicity implied by Eq. (1) of period in $\frac{2\pi}{n}$ ($n = \infty$ and $n = 1$), we expect reflection symmetry of the integer number of subbands at $\frac{2\pi}{n} = \pi$ or $n = 2$. We can therefore identify $n = 1$ with $n = \infty$, and trace the gaps back towards $n = 2$, with decreasing integer n as a complete mirror image of the left portion of the flux corresponding to $n = 2$. Thus, although reminiscent of Cantor set this cyclic characteristic, among others, of the Hofstadter butterfly spectrum then gives a diametrical contrast to the iterative construction of the Cantor set.

3.2 IQHE and FQHE Labelling

One most notable characteristics of the Hofstadter butterfly is the reconstruction of the topmost subband as well as that of the lowest subband. Although the left and right portion of the spectrum can be characterize as regions of IQHE regions [6, 7, 8], the top and bottom regions of the spectrum can be identified with the phenomenon of FQHE, since obviously this involves the reconstruction of a single subband [3] at high magnetic fields . This reconstruction is evidenced by the measurements [9, 10, 11] and Chern-Simons theoretical explanation of the FQHE given by Buot [3]. These are all indicated in Figs. (2) and (3).

4 CONCLUDING REMARKS

We need to say something about the profile of the *top* boundary of the *topmost* subband, as well as the *bottom* boundary of the *lowest* subband. The bottom profile of the lowest subband boundary must of the form of a convex curve with endpoints connecting the point $(0, 0)$ and $(1, 0)$. Similarly, the profile of the top boundary of the topmost subband must be a concave curve with endpoints at $(0, 1)$ and $(1, 1)$. This the main reason for the butterfly profile of the spectrum. This is reminiscent of the Landau levels shifting the lowest energies to higher energies, and the highest energy to lower energies in the presence of magnetic flux, reflecting the increase of $\hbar\omega = \frac{eB}{mc}$ without changing the total energies, since the magnetic field does not work on the system. This aspect of the spectrum is indicated in Figs. (2) and (3).

Acknowledgement 1 *The author is grateful for the 'Balik Scientist' Visiting Professor grant of the PCIEERD-DOST, Philippines, at Cebu Normal University, Cebu City, Philippines.*

References

- [1] D.R. Hofstadter, *Energy levels and wave functions of Bloch electrons in rational and irrational magnetic fields*, Phys. Rev. **B14**, 2239 (1976).
- [2] G.H. Wannier, *A Result Not Dependent on Rationality for Bloch Electrons in a Magnetic Field*, Phys. Stat. Sol. (b) **88**, 757 (1978).
- [3] F.A Buot, G. Maglasang, A.R.F. Elnar, and C.M. Galon, *On Fractional Quantum Hall Effect (FQHE): A Chern-Simons and nonequilibrium quantum transport Weyl transform approach*, arXiv: 2107.13970 (2021).
- [4] T. Van Mechelen and Z. Jacob, *Viscous Maxwell-Chern-Simons theory for topological electromagnetic phases of matter*, Phys. Rev. B **102**, 155425 (2020).
- [5] Felix A. Buot, *On quantum Hall effect: Covariant derivatives, Wilson lines, gauge potentials, lattice Weyl transforms, and Chern numbers*, arXiv:2106.16238 (2021).
- [6] Felix A. Buot, *Nonequilibrium superfield and lattice Weyl transform approach to quantum Hall effect*, arXiv:2001.06993
- [7] Felix A. Buot, *Comments on the Weyl-Wigner calculus for lattice models*, <http://arxiv.org/abs/2103.10351>
- [8] Felix A. Buot, *On the quantization of Hall effect in electrical conductivity: A nonequilibrium quantum superfield and lattice Weyl transform transport approach*, AIP Conference Proceedings **2286**, 030007 (2020). *Quantum-Based Devices*, Phys. Rev. B **42**, 9429-9456 (1990).

- [9] Stormer, H. (1992). *Two-dimensional electron correlation in high magnetic fields*. Physica B: Condensed Matter, 177(14), 401-408.
- [10] R. Willett, J. P. Eisenstein, H.L. Stormer, D. C. Tsui, A. C. Gossard and J. H. English, *Observation of an Even-Denominator Quantum Number in the Fractional Quantum Hall Effect*, Phys. Rev. Letts. 59, 1776 (1987).
- [11] W. Pan, H. L. Stormer, D. C. Tsui, L. N. Pfeiffer, K.W. Baldwin, and K.W. West, *Fractional Quantum Hall Effect of Composite Fermions*, Phys. Rev. Letts. **90**, 016801-1 (2003).

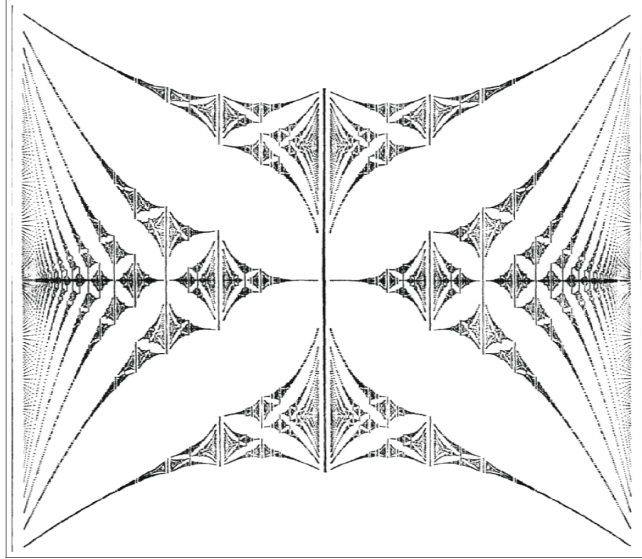


Figure 1: The Hofstadter butterfly energy spectrum obtained from computer graphics rendering of computer numerical simulation results. One characteristic feature is the wide band gap between topmost subband and lowest subband. This wide subband gap appears to allow the field to restructure the separated lower and upper central regions. Indeed, these two subbands are restructured left and right of the middle of the abscissa. [Figure taken from Hofstadter [1]]

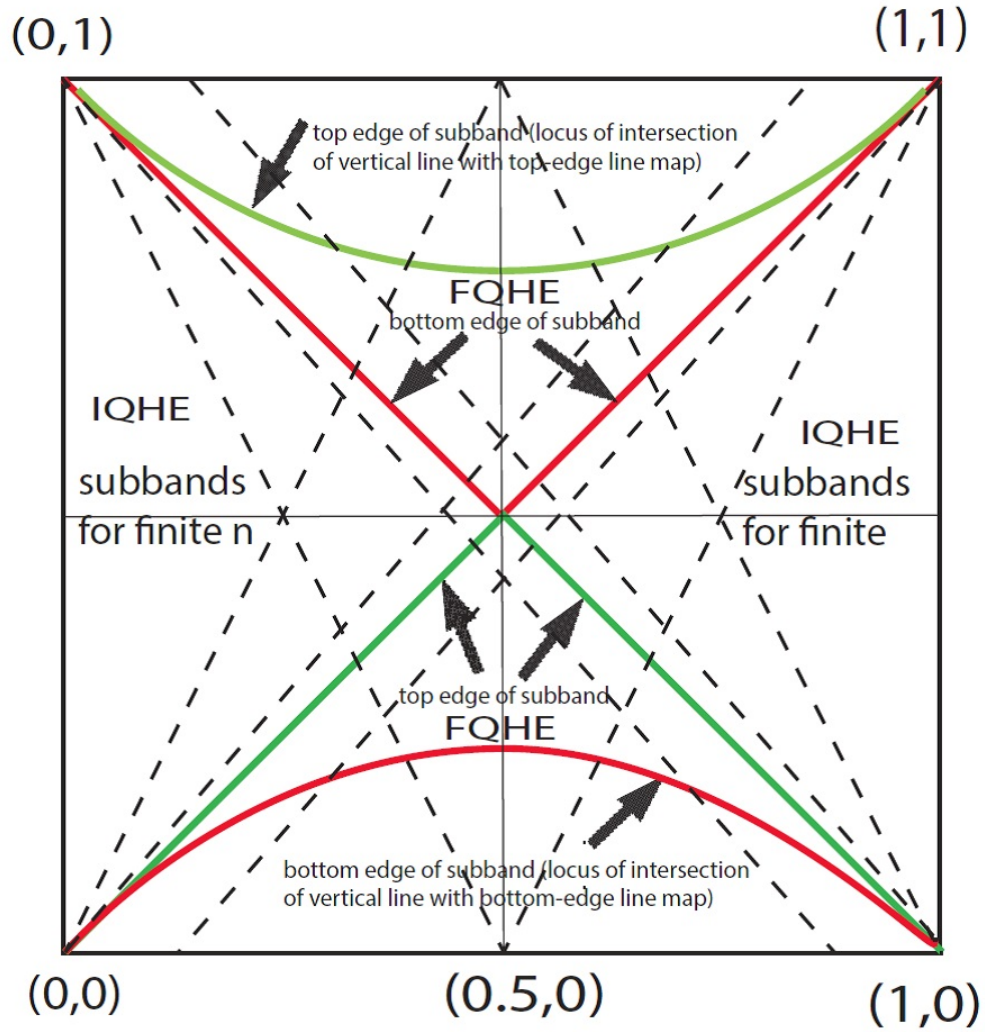


Figure 2: The lines in the figure map the center of the subband gaps. There are essentially four regions of the spectrum, separated by the diagonal lines. Remarkably, the diagonal lines represent wide subband gaps in Fig.1. The central lower and upper regions of the spectrum is counted as the first lower subband and the first upper subband, respectively. These two subbands clearly show up in the middle of the spectrum. However, to the left and right of the middle, these two subbands clearly undergo restructuring reminiscent of FQHE. Therefore, we label these two, lower and upper central regions, of the spectrum as the FQHE regions.

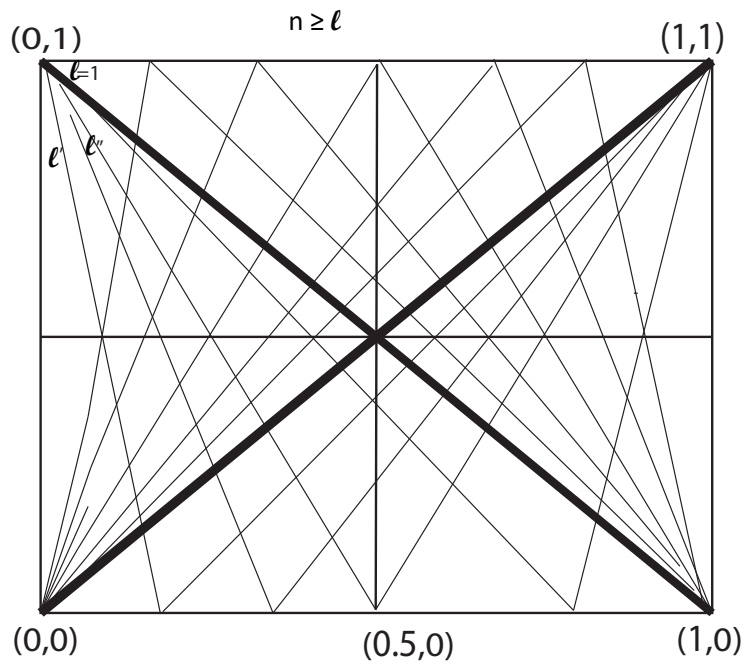


Figure 3: The figure shows how the lines emanates from the four corners of the spectrum.



Figure 4: An example of the iterative construction of a Cantor set. [Taken from Wikipedia]